Appl. Phys. A 67, 125–133 (1998)

Applied Physics A
Materials
Science & Processing

Invited paper

Phthalocyanine-C_{60} composites as improved photoreceptor materials?

B. Kessler

Forschungszentrum Jülich, IFF, D-52425 Jülich, Germany
(Fax: +49-2461/61-4037, E-mail: B.Kessler@fz-juelich.de)

Received: 16 March 1998/Accepted: 16 March 1998

Abstract. The electronic structure of phthalocyanine (Pc) materials, especially Cu−Pc, Fe−Pc, Ni−Pc, VO−Pc, TiO−Pc, and two modifications of H_2−Pc, in contact with C_{60} is studied using photoelectron spectroscopy with ultraviolet and X-ray radiation (UPS and XPS, respectively), X-ray absorption near edge spectroscopy (XANES), and optical transmission spectroscopy. A possible improvement of the charge-carrier generation efficiency, which is essential for the performance as photoreceptor material, is thereby found for these materials upon doping with C_{60}. No ground-state charge transfer is detected for the Pcs in contact with C_{60}. The effect of an enhanced photoconductivity is demonstrated for τ-H_2−Pc when it is doped by 5% C_{60}.

PACS: 79.60; 72.40

Organic photoconductors are of increasing importance for applications as photoreceptors for xerography or laser printers [1, 2]. They are less toxic than several inorganic compounds which are also in use for these purposes. Also, the properties of organic photoreceptors in terms of sensitivity for a specific spectral range can be designed as needed for special purposes. Diode-laser printers benefit from the absorption bands of phthalocyanines (Pcs) in the near infrared. A higher sensitivity or an increased speed in creating and transporting charges, on the other hand, could be very useful in order to expand the range of possible applications.

Figure 1a displays the working principle of a photoreceptor device for xerography or laser printing. The process starts with a charging of the surface by electrons. Positive image charges develop at the aluminium substrate. An illumination produces charge carriers via excited states in the charge-generation layer (CGL). The positive charges move through the hole-transporting charge-transport layer (CTL) and compensate the surface electronic charge creating thereby the image which then will be treated with toner, transferred to the paper and fused. Phthalocyanines, especially TiO−Pc or metal-free H_2−Pc are already in use in commercial CGL.

One of the key-needs of photoreceptor materials is a high efficiency for charge-carrier generation. This efficiency can be enhanced by lowering the recombination rate of excited states. Since a recombination is most likely directly after the excitation step, a fast charge separation should be able to decrease the recombination rate. In order to efficiently separate the charges a strong electron acceptor can be used (see Fig. 1b). The buckminsterfullerene C_{60} is an ideal candidate

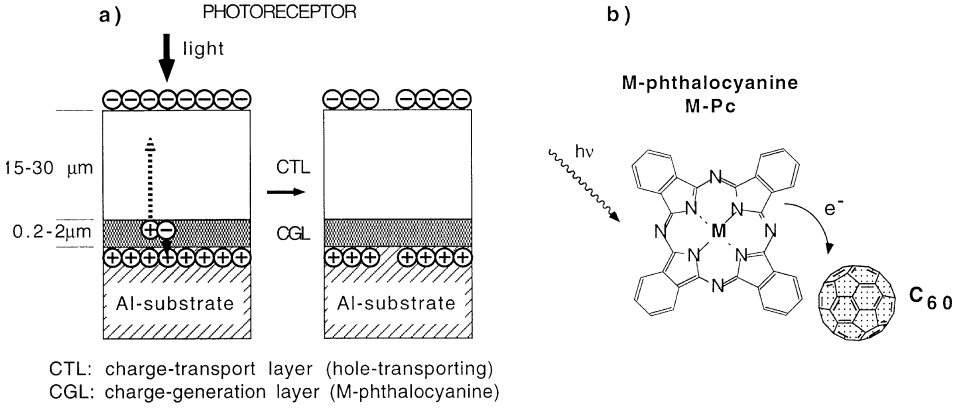

Fig. 1. a Principle of a photoreceptor device. **b** Model for the electron transfer from Pc to C_{60} after photoexcitation. M = Cu, Fe, Ni, VO, TiO, or H_2

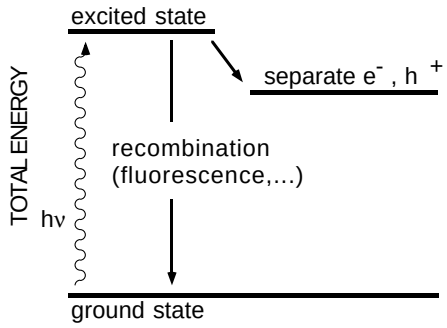

Fig. 2. Total energy scheme of photoexcited and charge-separated state (see text)

for this purpose since it is able to gather at least six electrons as in alkali-C_{60} compounds [3–5]. Therefore the idea is to mix it into conventional organic photoreceptors in order to increase their charge-generation efficiency. An unwanted enlargement of the dark conductivity is unlikely due to the rather high inertness of C_{60} towards chemical reactions.

However, a necessary condition for a successful charge transfer is that the charge-separated state is energetically preferred compared to the non-separated excited state (see Fig. 2). Therefore we study the electronic structure close to the optical gap of different Pcs in contact with C_{60} in order to determine the transition energy needed for an electron that is transferred from the valence band (VB) of the Pc towards the lowest unoccupied molecular orbital (LUMO) of C_{60}. Photoelectron spectroscopy with ultraviolet radiation (UPS) is used for the occupied states and information about the unoccupied states is obtained using X-ray absorption fine structure spectroscopy (XANES). Both methods are sensitive to possible chemical reactions of the components and therefore are used to estimate whether the dark conductivity may be enhanced in the compound compared to the pure Pc as a result of a possible ground-state electron transfer. The optical properties of the materials are checked by transmission spectra (200–1200 nm). A direct test of the effect of C_{60} as a doping material in Pcs is done by measurements of the photo- and dark current as a function of an applied voltage (I/U curves). Additional information about the geometrical order and the orbital character of sublimed Pc layers is obtained by angle-resolved photoelectron spectroscopy with polarized light (ARPES). In the following we will discuss these experimental results for various examples of Pcs.

1 Experimental

1.1 Sample preparation

Pcs were purchased from STREM-chemicals, C_{60} is used in a purity of 99.9%. "Model" samples are produced by sublimation from resistively heated Ta boats in ultrahigh vacuum (UHV) onto metal substrates or ITO-covered glass sheets. For the ARPES measurements a sputter-cleaned and vacuum-annealed Cu(100) single crystal is used as a substrate. Coverages are controlled with a quartz microbalance. After a thorough outgassing of the Ta boats in order to reduce the amount of solvents in the substances we deposit a rather thin layer of 100–300 Å Pc with the purpose of avoiding charging problems during the photoemission experiments. By this sublimation procedure the most stable configuration of the Pc is produced, which in the case of H_2-Pc is the α or β phase [1, 6]. In order to produce a sample of pure τ-H_2-Pc, material containing crystallites of this phase [7] needs to be drop cast from solution onto the substrate. C_{60} is UHV-sublimed from Ta boats in the coverage range of 0.5 up to about 6 monolayers (ML) for a study of the contact region between the fullerene and the Pc. 1 ML of C_{60} corresponds to 8 Å evaporated material with a density of $1.65\,\mathrm{g/cm^3}$ [8]. The sublimation technique is especially useful for the UPS and ARPES measurements since these methods are surface sensitive and the samples are kept under vacuum between the preparation and the analysis.

"Technical" samples were obtained from dispersions of the corresponding Pc and a resin binder, polyvinylbutyral (PVB) in toluene (AEG-Elektrofotografie). These samples are denoted as "technical" samples, because similar dispersions are used in the production process for CGL layers. The H_2-Pc that is used for this purpose has the τ configuration [1, 7]. A part of the material is mixed with about 5% (by weight) C_{60} before the sample is either drop cast or dip coated from the dispersion onto a metal or glass substrate. The samples for the optical transmission measurements, for the I/U measurements, and for some of the XANES measurements were prepared by this technique. A typical sample thickness for I/U measurements is 350 nm. These samples are sandwiches on a glass substrate with an indium–tin oxide (ITO) contact at one side and an evaporated Au contact at the surface. The contact area is about $0.5\,\mathrm{cm^2}$. In order to avoid systematic changes due to variations in the Au contacts, samples with and without C_{60} were treated as pairs when evaporating the Au contact.

1.2 UPS, XPS

After the preparation the samples are kept at room temperature under UHV and analyzed by photoelectron spectroscopy using a He-resonance light source (21.2 eV) for valence-band spectroscopy with ultraviolet radiation (UPS) or using monochromatized Al–K_α radiation (1486.6 eV) for core-level spectroscopy with X-rays (XPS). The photoelectrons are measured using a hemispherical analyzer with an angular acceptance of $\pm 8°$ in normal-emission geometry. All photoelectrons come from within an area of about 7 mm by 4 mm. The overall energy resolution is about 0.15 eV for UPS and 0.5 eV for XPS. The energy scale is referenced towards the Fermi level (E_F) of a bulk Au sample. XPS gives mainly information on the elemental composition of the samples; by UPS the valence levels that are directly involved in the chemical bonds are analyzed. The valence-band onset also is measured by UPS.

1.3 XANES

X-ray absorption near edge spectra (XANES) are taken using synchrotron radiation from the HE-PGM 3 monochromator at the electron storage ring for synchrotron radiation (BESSY) in Berlin. With this technique a core-level electron is excited into the unoccupied states at the same atom where the

core level is located. The excitation cross section depends on the density of unoccupied states. Measuring the secondary electron yield, which is proportional to the excitation cross section, as a function of the photon energy therefore gives the unoccupied density of states. The electrons are counted with a yield detector either collecting the total yield or the partial yield of electrons with kinetic energies above 20 eV. By using the partial yield the information depth is limited, because the very low kinetic energy electrons with a higher propagation length through the material, which dominate the total yield, do not contribute to the signal. The energy resolution depends on the photon energy and corresponds to about 0.3 eV at the C-1*s* absorption edge. The analyzed area is about 2 mm^2 and is determined by the synchrotron beam diameter on the sample. The spectra are taken either with normal light incidence or with an angle of about 45° between the light incidence and the sample surface.

1.4 ARPES

Angle-resolved photoelectron spectra (ARPES) are measured at the undulator beamline U2 at BESSY. The spectra are taken with grazing-light incidence (75° relative to the sample normal) and normal electron emission. The light polarization is chosen either with the polarization vector in the plane that contains the surface normal and the light incidence direction (p-polarized, see Fig. 3) or with the polarization vector perpendicular to this but in the surface plane (s-polarized). The photoelectrons are analyzed with a hemispherical analyzer with an angle resolution of ±5° in normal emission mode. The energy resolution is better than 0.1 eV. By the polarization dependence of the ARPES spectra information on the orientation and the type of molecular orbitals can be obtained [9, 10].

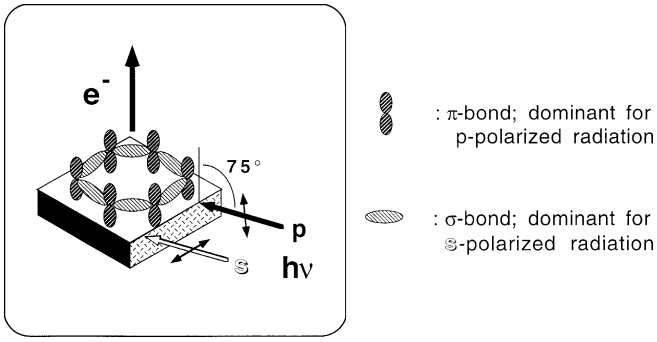

Fig. 3. Geometry of the ARPES spectra. Some π- and σ orbitals of a flat-lying C ring are given as an example; *s* and *p* denote the light polarization (see text)

1.5 Optical transmission spectra

Transmission spectra in the spectral region between 200 and 1200 nm are recorded from technical samples using a UV/VIS spectrometer. The sample thickness is about 350 nm as calculated from the optical properties under different angles of incidence. Different modifications of Pc can be distinguished by their typical transmission or absorption features [1, 7, 11]. Also, the energy of the optical gap can be estimated by this spectroscopy. However, an absorption across the optical gap does not directly produce free charge carriers, since this excitation creates singlet excitons in the first step [12]. Changes in the optical spectra upon doping with C_{60} help to identify a possible ground-state electron transfer.

1.6 I/U curves

The dark current and the photocurrent of sandwiches with glass/ITO/organic photoconductor/Au are investigated applying voltages between −0.1 V and 0.1 V by a Knick constant-voltage supply. The current is detected using a Keithley electrometer. The photocurrent is measured under illumination of the whole sample with monochromatic light at 610 nm from the glass/ITO side. The light intensity is about 16 μW at the sample surface. By this method a possible improvement of the photoconductivity properties of Pcs due to the influence of C_{60} can be directly tested.

2 Results and discussion

2.1 Growth modes

Phthalocyanines form molecular crystals upon evaporation. Different modifications are known that vary with respect to the distance between the stacked molecules and the angle between the molecular axis and the stacking direction. These modifications have typical absorption spectra and can be distinguished by using diffraction methods. Their performance as photoreceptor materials may be different [1, 7]. With our ARPES spectra we are able to shed some light on the way in which Pcs grow on a surface. Figure 4 shows ARPES spectra of Fe−Pc on Cu(100) for two different polarization directions (filled and open symbols) of the incoming synchrotron radiation. The photon energy is $h\nu = 100$ eV. The geometry is described in Fig. 3 (see also Sect. 1.4). The spectra are compared to an UPS spectrum taken with a He lamp (solid line, $h\nu = 21.2$ eV, substrate: Ta). The energy scale is referenced to the peak at the lowest binding energy, and the peaks are denoted A to E with increasing binding energy. For π levels the cross section decreases more strongly with increasing photon energy than for σ levels. An average between the two polarization-dependent spectra results in peak B being the strongest feature at $h\nu = 100$ eV. At the lower photon energy of 21.2 eV peak B is smaller compared to the other peaks suggesting that B is σ derived whereas the other strong peaks have π character. Although the character of peak A is not completely clear from our data it has been described as π derived by other authors [6, 9, 10, 13–15].

A clear difference in the relative intensities of the subsequent peaks for *s*- and *p*-polarized light is observed: peaks B and C are dominant for *s*-polarized light whereas the other peaks are strongest with *p*-polarization. Using the rather simple picture of the σ- and π bonds of a benzene molecule (see Fig. 3) as a model for the more complicated carbon rings in Fe−Pc (see inset in Fig. 4) we come to the following conclusion. Since the signal is strongest when the polarization vector points in the same direction as the maximum orbital amplitude we can conclude that the molecules lie rather flat

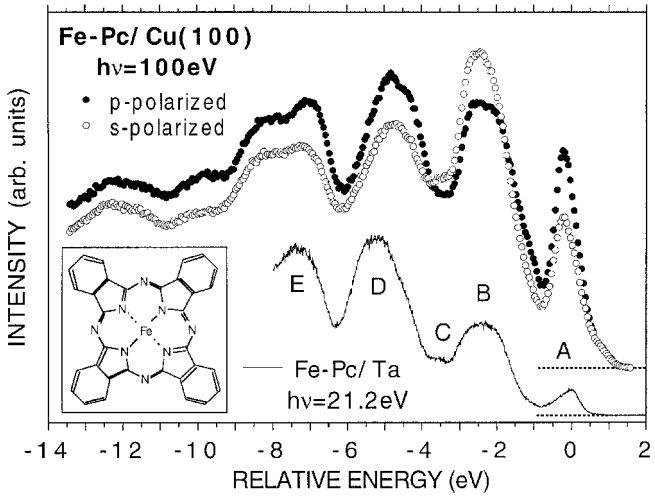

Fig. 4. Photoelectron spectra of Fe−Pc at different photon energies. The solid line is a UPS spectrum measured with a He lamp. Filled and open symbols denote the light polarization (p and s, respectively) of the ARPES spectra at $h\nu = 100$ eV. The binding energy scale is referenced to peak A. The inset shows a model of Fe−Pc

on the surface and peaks B and C contain σ symmetry, the other peaks are mainly π derived. If in contrast we would assume that the molecules "stand up" with arbitrary orientations relative to the incoming light the spectra would result in a dominance of the σ derived structures for p-polarization and roughly equal intensities for σ- and π features with p-polarized light. This is in contradiction to the above discussed variations caused by different cross sections at different photon energies. Although other orientations have been experimentally found for other combinations of Pcs and substrates, flat lying molecules seem to be quite common for monolayer coverages (see [9, 10] and references therein). Cu−Pc has been found to grow flat monolayers on Si(111) but randomly oriented monolayers on Si(001), which has been attributed to a weaker interaction between the adsorbate molecule and the Si(001) substrate [16]. The monolayer orientation has not been found to influence the tilt angle of the molecules within the molecular crystals for higher coverages [16]. Accordingly we found no influence of the underlying metal substrate on the spectral features of higher coverages of different M−Pcs.

2.2 Band alignment

Figure 5 displays a series of UPS spectra of Fe−Pc with increasing coverages of C_{60} (top to bottom). Since UPS has a very low information depth we focus here on the contact region between the Pc and the fullerene. With increasing binding energy (referenced to the Fermi energy) we denote the Fe−Pc peaks as A to E (in agreement with Fig. 4), the fullerene levels are numbered 1 to 4. 4 ML of C_{60} (bottommost spectrum) almost perfectly cover the structures of the underlying Fe−Pc and show some typical features of C_{60} [17]. A small remnant of peak A is still visible, but most of this feature is now attributed to a satellite of the He−I radiation with $h\nu = 23.08$ eV that causes a duplication of peak 1 at this binding energy. At lower coverages of C_{60} (0.5, 1, and 2 ML) the spectra can be interpreted as a simple superposition of features from both materials; no additional peaks can

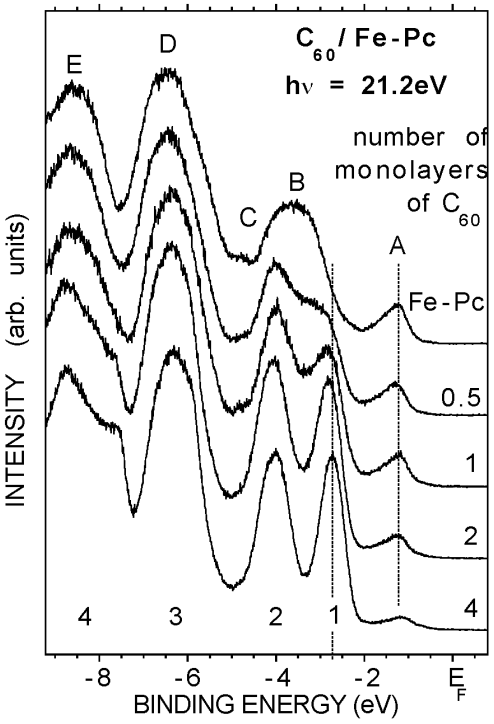

Fig. 5. Series of UPS spectra of Fe−Pc with increasing amount of C_{60}. The coverage is given in monolayers of C_{60}. Characters and numbers denote the features of Fe−Pc and C_{60}, respectively. The binding energy scale is referenced to the Fermi energy

be detected. This is even more clear when we try to produce a simulated spectrum from a superposition of a pure Fe−Pc and a pure C_{60} spectrum and compare this to the measured spectrum of 0.5-ML C_{60} on Fe−Pc. Figure 6 proves that a mixture of 70% Fe−Pc features and 30% C_{60} features almost perfectly reproduces the measured spectrum. No additional peaks and no broadening of the C_{60}-derived features close to E_F point towards a possible chemical reaction of both components. Therefore our conclusion is that no hybridization of the electronic states and thus no ground-state

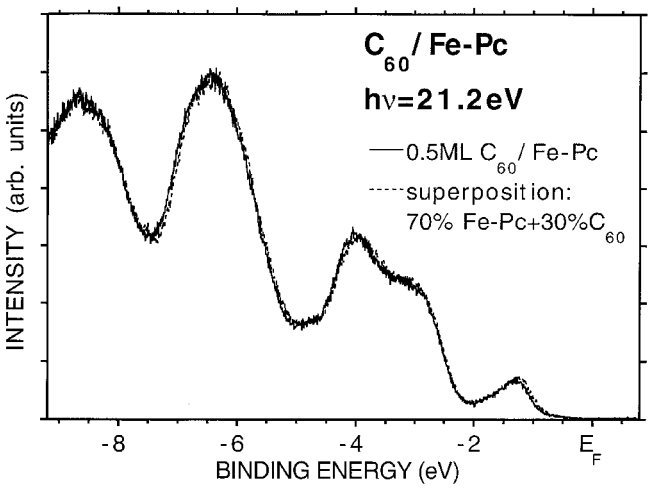

Fig. 6. Comparison of the measured UPS-spectrum of 0.5-ML C_{60} on Fe−Pc from Fig. 5 (*solid line*) with a constructed spectrum (*broken line*) composed from 70% of a pure Fe−Pc and 30% of a pure C_{60} spectrum. The binding energy scale is referenced to the Fermi energy

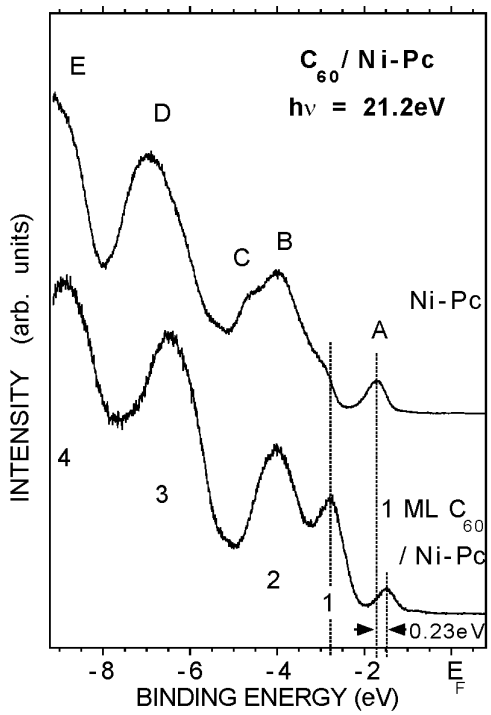

Fig. 7. UPS spectra of Ni−Pc and 1 ML of C_{60} on Ni−Pc. Characters and numbers denote the features of Ni−Pc and C_{60}, respectively. The binding energy scale is referenced to the Fermi energy

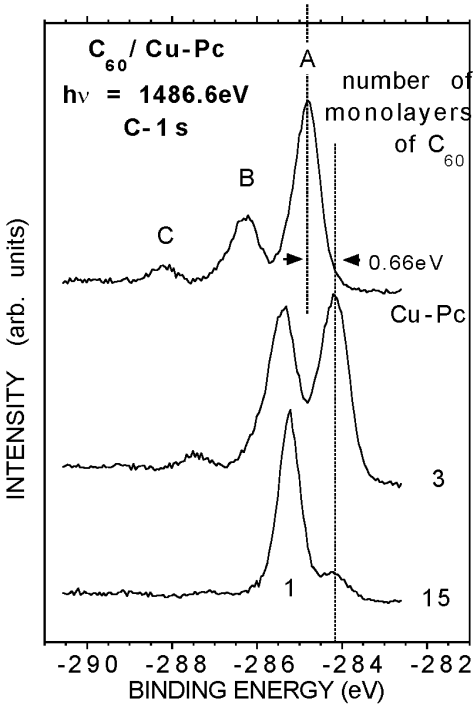

Fig. 8. XPS spectra of the C-1s peaks of Cu−Pc and increasing amounts of C_{60} on Cu−Pc. The binding energy scale is referenced to the Fermi energy. The Cu−Pc derived peaks (A, B, C) shift by 0.66 eV towards lower binding energies upon contact with C_{60}. Peak 1 is the C-1*s* peak of C_{60}

electron transfer takes place between Fe−Pc and C_{60}. This means that no enhancement of the dark current of Fe−Pc is expected when the material is mixed with C_{60}. The same result is obtained for similar simulations using the UPS spectra from Cu−Pc, Ni−Pc, VO−Pc, TiO−Pc, and H_2−Pc (not shown). All Pcs measured so far build stable interfaces with C_{60} in contrast to the observations concerning the polymer poly(3-octylthiophene), P3OT, with C_{60} [18]. The signal intensity of the C_{60}-derived features has been found to decrease within minutes for a room-temperature sample of C_{60} on P3OT. Cooling of the sample significantly reduces the spectral changes. A comparison of the more surface-sensitive UPS data to the more bulk-sensitive XPS data shows that the C_{60} diffuses into the polymer matrix [18]. We attribute this to the rather loosely bound polymer chains in P3OT. Molecular crystals of Pc on the other hand show no such behavior with C_{60} thereby proving a more closed structure which allows a stable interface between both components.

One difference although can be found for M−Pcs with differing M combined with C_{60}. Using, for example, M = Ni, Cu, TiO, or the metal-free H_2−Pc all Pc-derived features in the UPS spectrum shift on the binding energy scale towards the Fermi energy upon contact with C_{60}. This shift corresponds to 0.23 ± 0.15 eV for Ni−Pc (see Fig. 7) and 0.65 ± 0.15 eV for Cu−Pc [18], which can be seen most clearly for peak A in Fig. 7. Similar shifts can be observed in the Pc-derived features of the core levels of the corresponding materials upon contact with C_{60} measured by XPS spectra, independent of whether the core levels are C-1*s*, N-1*s*, or belong to the metal. An example is given in Fig. 8 where the C-1*s* core levels of Cu−Pc shift by 0.66 ± 0.15 eV upon evaporation of 3-ML C_{60}. We attribute these shifts to a change of the surface-band bending of the Pc-derived features when the surface is covered by C_{60}. Such a band-bending zone typically extends up to several hundreds of Å from the surface into the bulk [19]. Due to the low information depth of XPS and UPS only the shifted region close to the surface is analyzed. No information on the energy position of the levels deep inside the material can be obtained. This interpretation of a band bending is further supported by the fact that for different samples of Ni− and Cu−Pc also smaller values of the shift energies have been observed; the "final" positions of the peaks in contact with the fullerene on the other hand are always reproducible. Therefore we think that the differences in the "starting conditions" are due to different surface contaminations of the individual Pc surface, which influence the size of the surface band bending. The amount of these contaminations is too low to be confirmed by UPS or XPS. A contact with C_{60} on the other hand represents a well-defined situation where the bending conditions always are the same. A summary of the band-bending-induced shifts for the various Pcs is given in Table 1. This observation of a change of the surface-band bending concerning several M−Pcs upon contact with C_{60} demonstrates that it is not sufficient to measure the spectral features of the single components separately. Only a measurement of the two components in contact with each other gives the true values for the energy difference between the valence-band onset of C_{60} and the different M−Pcs.

2.3 Energetics of charge transfer

In order to know whether a charge transfer from an excited state of a specific type of Pc to C_{60} is possible, we need to determine the relative energy positions of the band offset between the corresponding Pc and the LUMO of C_{60}. From the

Table 1. Change of surface-band bending of different Pcs induced by C_{60} obtained from the UPS and XPS data (left column). Energy separation between the top of the valence band (VB onset) of different Pcs and the HOMO (middle column) and LUMO (right column) of C_{60} as deduced from Fig. 10

Material	Maximum value of band-bending shift /eV	Energy separation between VB onset of Pc and HOMO of C_{60} /eV	Minimum energy to transfer an electron from VB of Pc into LUMO of C_{60} /eV
TiO−Pc	0.1	1.1	1.2
α, β-H_2−Pc	0.25	1.1	1.2
τ-H_2−Pc	0.25	1.3	1.0
VO−Pc	0	1.2	1.1
Ni−Pc	0.23	1.15	1.15
Fe−Pc	0	1.4	0.9
Cu−Pc	0.65	1.5	0.8

UPS spectra the energy separation between the VB of the Pc and the HOMO of C_{60} can be obtained. We therefore shift the spectra of pure Pcs by the value of the band-bending shift towards the Fermi energy; this is the position which the Pc levels have when the Pc is in contact with C_{60}. Also the additional intensity from the contribution of the He-1_β radiation at $h\nu = 23.08$ eV (2.5%) to the UPS spectra of the pure Pc and the pure C_{60} has to be subtracted. Figure 9a displays the resulting spectra for pure Ni−Pc and C_{60} as an example. An extrapolation of the peak flanks towards the background intensity gives the value for the valence-band onset of Ni−Pc and the top of the HOMO of C_{60}. Using the published value of 2.3 eV for the band gap of C_{60} [20] a schematic of the bands which are relevant for a charge transfer is obtained (see Fig. 9b). From this schematic it can be deduced that an electron needs an energy of 1.15 eV in order to be transferred from the top of the valence band of Ni−Pc to the LUMO of C_{60}. If this process involves an excited state of the Pc, like an exciton, this excited state has to supply the necessary energy (compare Fig. 2). The optical absorption of Ni−Pc has its lowest-energy maximum at a photon energy of about 1.8 eV reaching half of its intensity around 1.7 eV [21–23]. Therefore from energy considerations a transfer of the electron into the LUMO of C_{60} should be possible.

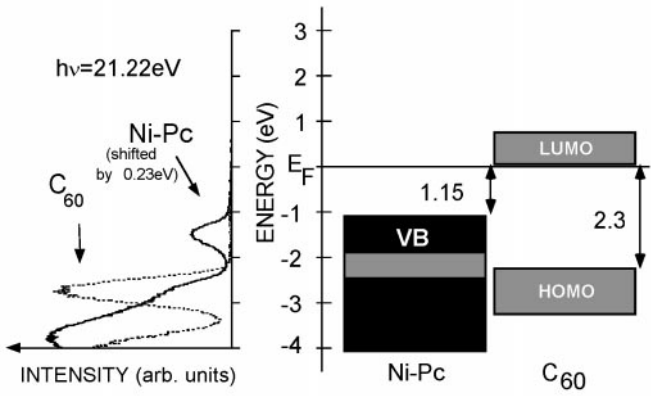

Fig. 9. a Relative energy positions of UPS features of Ni−Pc and C_{60} in the mixed material. **b** Energy scheme of Ni−Pc and C_{60} in the region of the optical gap

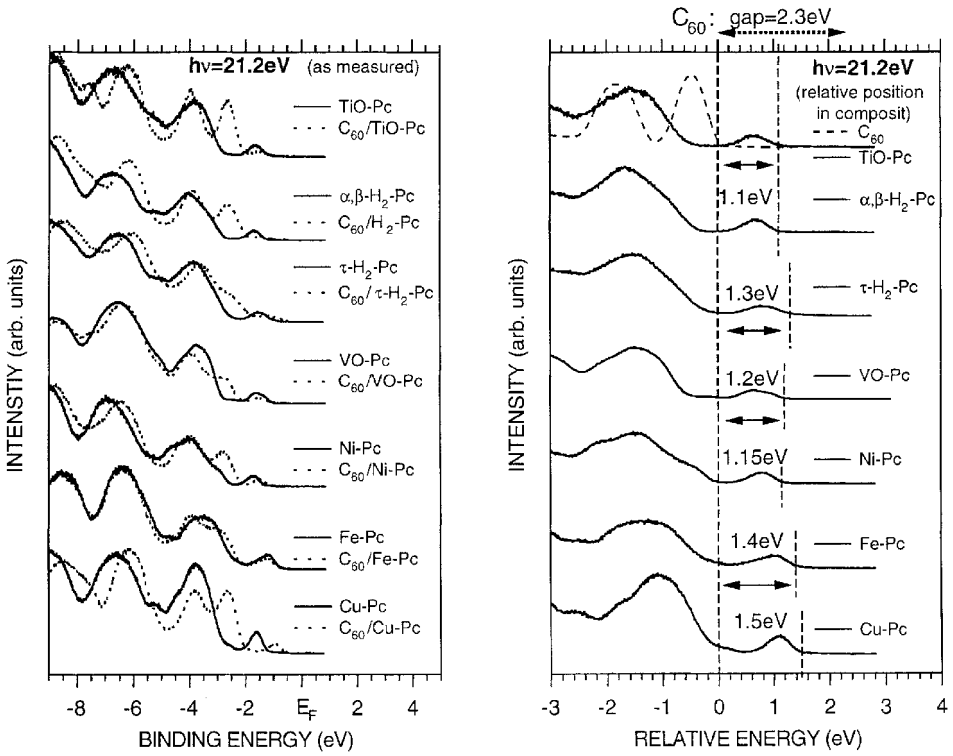

Fig. 10. (left) Intensity-normalized UPS spectra of different Pcs (*solid line*) and thin layers of C_{60} (*broken line*) on the corresponding Pc. The energy scale is referenced to the Fermi energy. (right) Relative energy of the VB onset of the Pcs in comparison to the position of the HOMO of C_{60} in the mixed material derived from the spectra in the left panel (see text). The energy scale is referenced to the top of the HOMO of C_{60}

Equivalent band schemes can be extracted from the UPS spectra of the other Pcs in contact with C_{60}. The left panel of Fig. 10 shows the spectra of the different Pcs in comparison to the same materials with thin overlayers of C_{60} (as measured). In the right panel the normalized contributions from both components (Pc and C_{60}) to the overlayer spectra are displayed on a common energy axis where 0 eV corresponds to the top of the HOMO of C_{60}. From these spectra the energy separation of the individual Pc valence-band onset to the top of the HOMO of C_{60} can be obtained (Fig. 10 right panel). The difference between the gap size of C_{60} (2.3 eV) and this energy separation yields the energy which is needed to transfer an electron from the VB of the Pc to the LUMO of C_{60}. The results are displayed in Table 1. This energy value has to be compared to the amount of energy that has been deposited in the photoreceptor system by the optical excitation.

The maxima of the typical optical absorption energies of the different Pcs range between 1.5 eV (for VO−Pc) and 1.8 eV (for Ni−Pc) [1, 7, 11, 21–24]. Such an optical excitation creates a singlet exciton on the excited Pc molecule. This is a bound state and does not correspond to free charge carriers. For example, in the case of metal-free H_2−Pc the corresponding singlet excitation energy is 1.65 eV, but the energy of the band gap is 2.08 eV [25]. The excited system may lose some of its energy by different mechanisms including internal conversion into lower-lying singlet states, creation of a charge-transfer exciton involving a neighbor molecule, or by intersystem crossing into a triplet excitonic state. For higher light intensities even nonlinear processes may occur such as annihilation between two excitons of the same kind [26]. All of theses processes have different timescales for the different M−Pcs that even depend on the spin–orbit interaction of the central element [27]. Usually the singlet decays much faster than the triplet. We nevertheless consider both levels here as possible precursors for an electron transfer into the LUMO of C_{60}. As a rough estimate the energy difference between the first excited triplet level and the ground state is about two-thirds of the first singlet excitation energy [28]. Since most of the Pcs are rather similar we take the value of 1.1 eV for the lowest-energy triplet excitonic level of Zn−Pc [29] as a measure for typical triplet excitons of Pcs. Therefore on one hand, an electron transfer from a triplet excitonic state of Cu−Pc, Fe−Pc, VO−Pc, and τ-H_2−Pc into the LUMO of C_{60} is possible, since 0.8 eV, 0.9 eV, 1.0 eV, and 1.1 eV are needed, respectively, and the excitonic state is able to supply 1.1 eV. For Ni−Pc, TiO−Pc, and α, β-H_2−Pc on the other hand, it is unlikely that such a process will occur. It is quite interesting that the two modifications of H_2−Pc behave differently in this context.

2.4 Unoccupied states and charge transfer

The XANES spectra give some additional insight into the situation of the unoccupied orbitals. As an example we pick the XANES spectra of Fe−Pc and Ni−Pc with C_{60}. The inset in Fig. 11a displays the spectrum of pure Fe−Pc (solid line in inset) and the spectrum of 0.5-ML C_{60} on Fe−Pc (broken line in inset) in the photon energy region where an excitation from the C-1*s* core level into the unoccupied density of states takes place. The spectra of the pure Fe−Pc correspond well to previously published data. The lowest energy peak and shoulder belong to a $1s \rightarrow \pi^*$ resonance [30]. If we take a weighted difference between both spectra we almost perfectly reproduce a pure C_{60} XANES spectrum (broken line in main frame of Fig. 11a). The high symmetry of C_{60} results in a rather sharp $1s \rightarrow \pi^*$ resonance peak around $h\nu = 284.3$ eV, which is typical for C_{60}. These π orbitals are quite sensitive to any chemical reaction and therefore provide a good test. No additional features and no peak broadening can be detected demonstrating that the unoccupied levels do not participate in any possible chemical reaction, which is consistent with the absence of a ground-state charge transfer between the different components of the sample. Similar results are obtained for Ni−Pc (see Fig. 11b), Cu−Pc, TiO−Pc, and VO−Pc with C_{60} (not shown). XANES spectra at photon energies where N-1*s* or the corresponding metal electrons are excited do not show any change at all upon contact of the Pc with C_{60} (besides a trivial reduction of the intensity due to the C_{60} overlayer). Even no energy shift can be detected. This indirectly confirms the above interpretation of the shifts in the XPS and UPS spectra of Cu−Pc, Ni−Pc, TiO−Pc, and

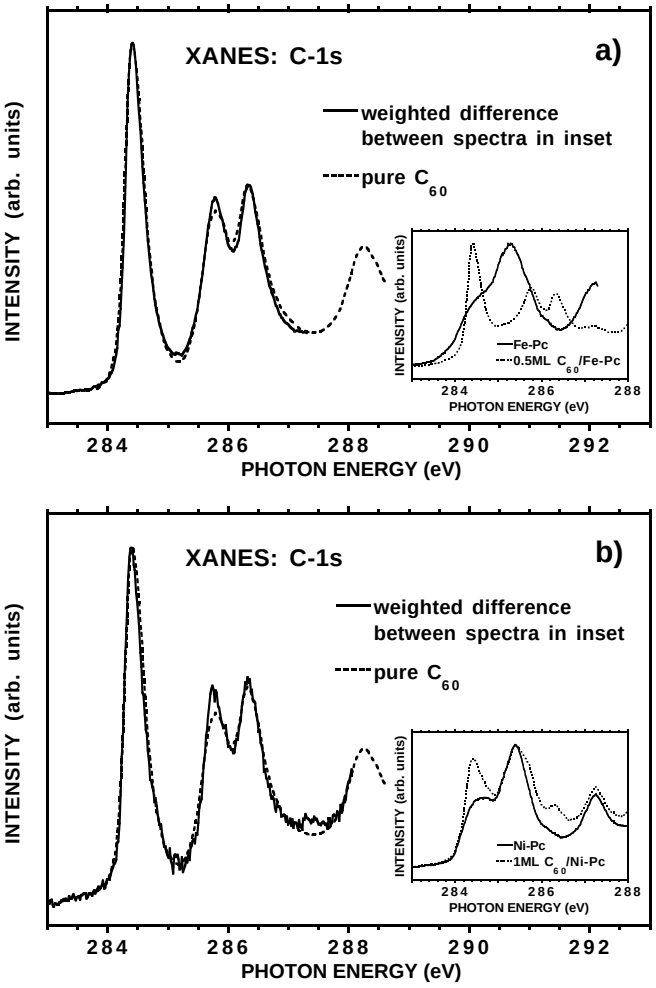

Fig. 11. a Inset: XANES spectra at the C-1s edge of Fe−Pc (*solid line*) and 0.5 ML of C_{60} on Fe−Pc (*broken line*). Main frame: measured spectrum of pure C_{60} (*solid line*), constructed spectrum (*broken line*) from a weighted difference of the spectra in the inset. **b** Inset: XANES spectra at the C-1s edge of Ni−Pc (*solid line*) and 1 ML of C_{60} on Ni−Pc (*broken line*). Main frame: measured spectrum of pure C_{60} (*solid line*), constructed spectrum (*broken line*) from a weighted difference of the spectra in the inset

τ-H_2−Pc to be due to surface-band bending; since all levels are shifted, a measurement of the energy separations (as done by XANES) is expected to reveal no change. Unfortunately the relative positions of the unoccupied levels of the Pc and C_{60} cannot be deduced from the XANES spectra because the amount of excitonic energy between the core-level hole and the excited electron is unknown and may be different for each compound.

XANES is an ideal tool to study technical samples, for example τ-H_2−Pc, with binder material and C_{60}. These samples cannot be analyzed using UPS because of the higher surface sensitivity of UPS. A part of the problem is caused by surface contaminations due to the preparation outside of a vacuum chamber, also the C_{60} is diluted deep inside the sample. A method that is restricted to the very few surface layers, such as UPS, does not give much information on it. The main panel of Fig. 12 displays the XANES results from a technical sample composite (solid line) based on τ-H_2−Pc and binder with an admixture of 5% C_{60}. The spectrum can almost be perfectly reproduced by a superposition (broken line) of the spectra of the single components (see inset). This is especially remarkable since the pure H_2−Pc spectrum corresponds to α, β-H_2−Pc. This clearly demonstrates that the three components of the sample do not undergo any chemical reaction or ground-state charge transfer. Therefore we do not expect an enhanced dark conductivity of H_2−Pc with binder upon an admixture of C_{60}.

A chemical reaction between C_{60} and H_2−Pc will also change the features of the optical absorption spectrum. Figure 13 shows a comparison of the optical spectra of technical samples of τ-H_2−Pc and binder without and with C_{60}, (thin solid line and broken line, respectively). There is only a minor difference in the transmission features caused by the C_{60} which coincides with the main features of pure C_{60} in the optical density [31]. No additional features are detected, which is quite in accordance with the results from the XANES spectra (see above) that no ground-state charge transfer is found. The optical transmission data of the sublimed α, β-H_2−Pc phase, on the other hand, differ significantly from the features

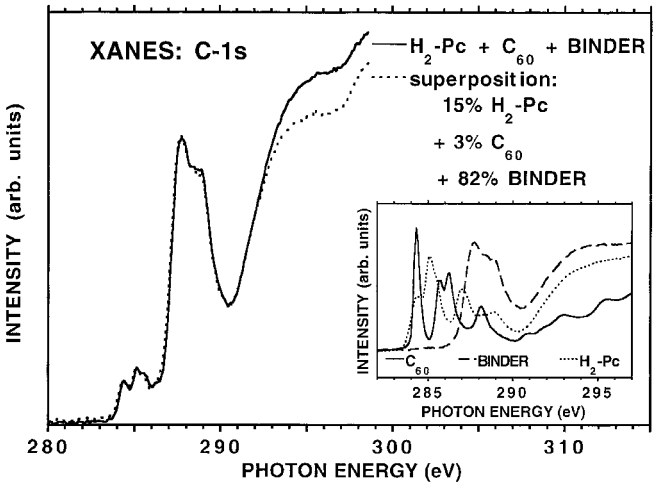

Fig. 12. Inset: XANES spectra at the C-1s edge of pure C_{60} (*solid line*), pure binder (*dashed line*) and pure α, β-H_2−Pc (*broken line*). Main frame: measured spectrum (*solid line*) of a mixed technical sample containing τ-H_2−Pc, binder and C_{60}, constructed spectrum (*broken line*) from a superposition of the spectra in the inset

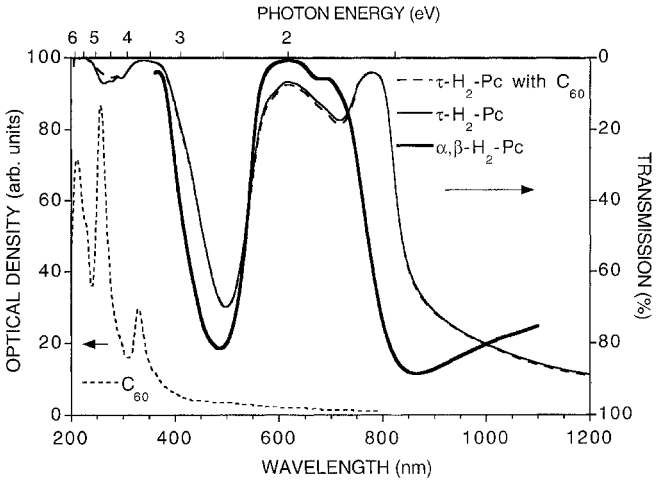

Fig. 13. Optical spectra of technical sample composites of τ-H_2−Pc and binder with (*broken line*) and without C_{60} (*thin solid line*) and a sublimed model sample of α, β-H_2−Pc (*thick solid line*) measured in transmission technique (*right scale*) for wavelengths between 200 and 1200 nm. The dashed line gives a spectrum of the optical density of pure C_{60} for comparison (*left scale*) measured by UV/Vis [31]

of the τ phase [7]. The optical gaps (half intensity of the maximum) correspond to about 1.6 eV and 1.5 eV, respectively.

2.5 Improvement of the photoconductivity

The improvement of a technical sample of τ-H_2−Pc with binder by C_{60} can be directly seen from the dark- and photocurrent measurements in Fig. 14. Panel **a** shows the photoconductivity of a technical sample of τ-H_2−Pc in comparison with a sample containing an admixture of 5% C_{60}. Both curves have been scaled in a way that the data points fit into the same window. A comparison of the left scale (photocurrent of τ-H_2−Pc) and the right scale (photocurrent of doped material) demonstrates that the doping enhances the photoconductivity by a factor of 20. Whereas the photocurrent of the pure material is about 4×10^{-10} A at 0.1 V it reaches 8×10^{-9} A for the doped sample. Panel **b** shows the results for the dark current of both samples. The ratio between the scale parameters of panel **a** and panel **b** thereby correlates to the contrast of the corresponding material. The contrast of about 100 for the τ-H_2−Pc improves to about 200 for the case of 5% C_{60} in τ-H_2−Pc. Therefore we can conclude that the doping enhances the photoconductivity and the contrast.

3 Conclusions

The influence of the buckminsterfullerene C_{60} on the electronic properties of different phthalocyanines, especially Cu−Pc, Fe−Pc, Ni−Pc, VO−Pc, TiO−Pc, and two different modifications of H_2−Pc, has been analyzed by photoelectron spectroscopy (ARPES, XPS, UPS), X-ray absorption fine structure measurements (XANES), transmission spectroscopy, and current/voltage curves (dark and illuminated by monochromatic visible light). Our results show that for all the Pcs studied here a charge separation of the singlet excitonic state is energetically possible when the material is doped with C_{60}. It is therefore expected that the

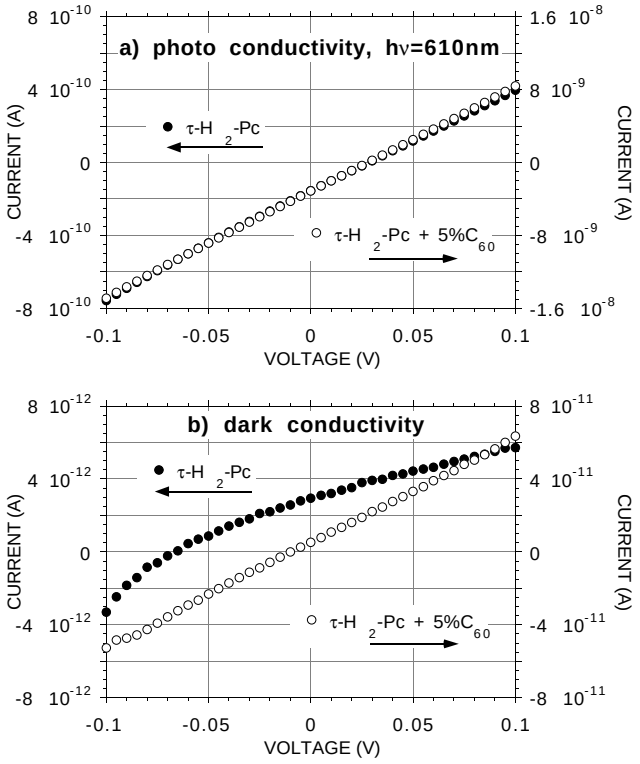

Fig. 14a,b. I/U curves of sandwiches of technical samples of τ-H_2-Pc and binder with (*open symbols*, *right scale*) and without C_{60} (*filled symbols*, *left scale*). The sample composition is: glass/ITO/τ-H_2-Pc composite/Au. The sandwich is grounded at the ITO contact; the voltage is applied at the Au-contact. **a** sample illuminated by radiation with a wavelength of 610 nm from the ITO side, **b** sample without illumination

luminescence will be quenched and the photocarrier generation will be improved. For Cu−Pc, Fe−Pc, VO−Pc, and τ-H_2-Pc even a charge separation of the triplet excitonic state is energetically possible, which might be a second path to improve the charge carrier generation. No improvement via triplet excitonic states is expected for Ni−Pc, TiO−Pc, and α, β-H_2-Pc with C_{60}. All the Pcs studied here build stable interfaces with C_{60}. No ground-state electron transfer was found, leading to the conclusion that the dark current is not expected to be greatly enhanced upon doping by C_{60}. For technical sample composites of τ-H_2-Pc with a polymeric binder that are already in use as photoreceptor materials, transmission spectroscopy results gave no indication for a ground-state electron transfer upon admixture of 5% C_{60}. An enhancement of the photoconductivity and an improved contrast between photocurrent and darkcurrent has directly been seen from the I/U curves for sandwiches of these materials between Au and ITO contacts when the H_2-Pc-binder composite is mixed with 5% C_{60}.

Acknowledgements. The project is supported by the BMBF-VDI via contract number 13N6906. B.K. acknowledges the financial support by the Ministerium für Wissenschaft und Forschung des Landes Nordrhein-Westfalen. The results would not have been possible without the contributions of C. Schlebusch, J. Morenzin, S. Cramm, L. Baumgarten, A. Scholl, and W. Eberhardt to the experimental work and the discussions. The dispersions for the technical samples have been kindly provided by M. Biermann and M. Lutz from AEG Elektrofotografie.

References

1. K.-Y. Law: Chemical Reviews **93**, 449 (1993)
2. P. DiMarco, G. Giro: In *Organic Conductors*, ed. by J.-P. Farges (Marcel Dekker Inc., New York 1994) p. 791
3. P.J. Benning, J.L. Martin, J.H. Weaver, L.P.F. Chibante, R.E. Smalley: Science **252**, 1417 (1991)
4. G.K. Wertheim, J.E. Rowe, D.N.E. Buchanan, E.E. Chaban, A.F. Hebard, A.R. Kordan, A.V. Makhija, R.C. Haddon: Science **252**, 1419 (1991)
5. P.J. Benning, F. Stepniak, J.H. Weaver: Phys. Rev. B **48**, 9086 (1993)
6. E. Orti, J.-L. Brédas: J. Am. Chem. Soc. **114**, 8669 (1992)
7. A. Kakuta, Y. Mori, S. Takano, M. Saweda, I. Shibuya: J. Imag. Techn. **11**, 7 (1985)
8. T.R. Ohno, Y. Chen, S.E. Harvey, G.H. Kroll, J.H. Weaver, R.E. Haufler, R.E. Smalley: Phys. Rev. B **44**, 13747 (1991)
9. T. Permien, R. Engelhardt, C.A. Feldmann, E.E. Koch: Chem. Phys. Lett. **98**, 527 (1983)
10. N. Ueno, K. Suzuki, S. Hasegawa, K. Kamiya, K. Seki, H. Inokuchi: J. Chem. Phys. **99**, 7169 (1993)
11. B.H. Schlechtman, W.E. Spicer: J. Mol. Spectry. **33**, 28 (1970)
12. J. Noolandi, K.M. Hong: J. Chem. Phys. **70**, 3230 (1979)
13. F.L. Battye, A. Goldmann, L. Kasper: Phys. Status Solidi B **80**, 425 (1977)
14. D. Guay, G. Tourillon, L. Gastonguay, J.P. Dodelet, K.W. Nebesny, N.R. Armstrong, R. Garret: J. Phys. Chem. **95**, 521 (1991)
15. S. Maroie, M. Savy, J.J. Verbist: Inorg. Chem. **18**, 2560 (1979)
16. G. Dufour, C. Poncey, F. Rochet, H. Roulet, M. Sacchi, M. De Santis, M. De Crescenzi: Surface Sci. **319**, 251 (1994)
17. J.H. Weaver, J.L. Martins, T. Komeda, Y. Chen, T.R. Ohno, G.H. Kroll, N. Troullier, R.E. Haufler, R.E. Smalley: Phys. Rev. Lett. **66**, 1741 (1991)
18. C. Schlebusch, B. Kessler, S. Cramm, W. Eberhardt: Synth. Metals **77**, 151 (1996)
19. K. Horn: J. Appl. Phys. A **51**, 289 (1990)
20. R.W. Lof, M.A. van Venendaal, B. Koopmans, H.T. Jonkman, G.A. Sawatzky: Phys. Rev. Lett. **68**, 3924 (1992)
21. P. Day, R.J.P. Williams: J. Chem. Phys. **37**, 567 (1962)
22. E.A. Lucia, F.D. Verderame: J. Chem. Phys. **48**, 2674 (1968)
23. H. Yoshida, Y. Tokura, T. Koda: Chem. Phys. **109**, 375 (1986)
24. L. Edwards, M. Gouterman: J. Mol. Spectrosc. **33**, 292 (1970)
25. Z.D. Popovic: Chem. Phys. **86**, 311 (1984)
26. M. Ichikawa, H. Fukumura, H. Masuhara, A. Koide, H. Hyakutake: Chem. Phys. Lett. **232**, 346 (1995)
27. W.F. Kosonocky, S.E. Harrison, R. Stander: J. Chem. Phys. **43**, 831 (1963)
28. F. Gutmann, L.E. Lyons: *Organic Semiconductors* (Wiley, New York 1967)
29. E.E. Koch: Phys. Scr. **17**, 120 (1986)
30. E.E. Koch, Y. Jugnet, F.J. Himpsel: Chem. Phys. Lett. **116**, 7 (1985)
31. J.P. Hare, H.W. Kroto, R. Taylor: Chem. Phys. Lett. **177**, 394 (1991)